Self-phase modulation and short-pulse generation from laser-breakdown plasmas

Eli Yablonovitch*
Bell Telephone Laboratories, Holmdel, New Jersey 07733
(Received 26 June 1974)

This paper is a complete report on both the experimental and theoretical aspects of the recently discovered self-phase modulation in laser-breakdown plasmas. Mainly responsible for these effects is the sudden index change which accompanies the ionization of the gaseous medium. Two theoretical models are introduced for the phase and amplitude modulation induced by the plasma. These effects are applied to the problem of short-optical-pulse generation, with emphasis on the prospects for producing a pulse consisting of only a few optical cycles. The techniques described here have the unique advantage that the generation mechanism is *linear*, resulting in particularly clean, reproducible and predictable optical transients. Methods are suggested for raising the plasma nucleation intensity by further cleaning up the gas. It is shown that index dispersion of the optical components may place a lower limit on pulse duration.

I. INTRODUCTION

Although laser-induced breakdown has been known since the early days[1] of high-power lasers, its importance to nonlinear optics was recognized only in the last few years. These strong nonlinear optical effects are due to the sizable index of refraction change Δn, which accompanies the ionization of an initially neutral medium.[2] Indeed, when the ionization density exceeds the critical density, the index of refraction drops to zero.[3] Therefore, the change in index $\Delta n \sim -1$, is extraordinarily large.

In this paper we will consider the self-broadening[4] and self-phase modulation[3] effects which are produced by high-intensity laser breakdown in clean gases. It will be shown how the optical switch based on the plasma cutoff may be used for short-pulse generation,[4] including the recently developed optical free-induction-decay pulse generator.[5] These techniques are unique in that the temporal pulse shape and duration are determined by linear optical filters. This is to be distinguished from techniques such as mode locking which depend on the nonlinear effects of saturable absorption and gain. Finally, we will explore the prospects for producing a light pulse consisting of only a few optical cycles, which would be the shortest duration ever.

II. THEORY

In a laser breakdown experiment in a gas, the focal volume resembles an explosive medium. Once the plasma is triggered, the neutral gas becomes rapidly ionized. The index of refraction drops from a nominal value of unity to a value of zero as the electron density N exceeds the critical density N_c. Thus the incident laser beam is being transmitted through a region of rapidly varying index $n(x,t)$, both in space and time. Here, $n(x,t)=[1-N(x,t)/N_c]^{1/2}$, where $N_c=m\omega^2/4\pi e^2$ is the critical density at which the plasma frequency equals the laser frequency.

In this paper we will be concerned mainly with the frequency spectrum of the light transmitted through the plasma region. Therefore, the light is acting as a probe of a plasma it has itself created. This is the reason for the use of the term *self*-phase modulation.

At various times during the growth period of the plasma, it will have four distinct effects on the beam transmitted through the focus: (a) It will absorb part of the beam, thereby modulating it in amplitude. (b) It will scatter part of the beam out of the forward direction, again reducing its amplitude. Since the light is generally focused by an $f/1$ lens, it should be remembered that the forward direction is actually a cone of half-angle ~30°. (c) It will scatter part of the beam into the forward direction, but with a phase shift caused by the plasma index being less than 1. (d) It will leave part of the beam unaffected.

At early times, before the plasma has nucleated, or while $N \ll N_c$ only (d) is important and the beam would be transmitted intact. Once the plasma has spread through the focal region, only (a) and (b) are important and the transmission would be completely cut off. At intermediate times, all four effects are important and the beam experiences both amplitude and phase modulation.

Since a complete solution of the wave equation for light scattering of a tightly focused beam off a plasma region of dimension approximately one wavelength is impossible, we will adopt a different approach. By taking account of the physical processes (a)–(d) we will attempt to model the phase and amplitude modulation induced by the plasma on the light beam.

III. MODEL (A)

Model (A) assumes a plasma which is spatially homogeneous throughout the focal region. It further assumes that the uniform plasma density is growing exponentially in time, as it would in an electron avalanche, i.e., $N(t)=N_0e^{t/T_a}$, where T_a is the avalanche growth rate.

We make the additional approximation $N \ll N_c$. This will be valid if the plasma becomes opaque due to linear absorption even before the electron density reaches the critical density. In this case the change in complex index of refraction $\Delta n(t)$ is simply proportional to the plasma density $N(t)$. The plasma shifts the phase of the wave by $\phi = -\Delta n(t) z\omega/c$, where z is the propagation path length. Using the familiar Drude model[6] for the plasma contribution to the real and imaginary parts of the refractive index, the phase shift becomes

$$\phi = \tfrac{1}{2}(\omega\tau - i)N(t)z\sigma, \qquad (1)$$

where τ is the electron collision time and σ is the free-electron absorption cross section. The imaginary part of ϕ represents absorption of the wave.

Figure 1(a) is a phasor diagram, appropriate to model (A), of the path of the electric field vector in the complex plane. As the plasma density increases, the phase shift builds up, and the electric vector goes around and around the origin of the complex plane. As the density $N(t)$ increases further, the imaginary part of ϕ becomes important, the wave is attenuated and the electric vector spirals into the origin. Since the real part of ϕ is $\omega\tau$ times greater than the imaginary part, the phasor will circle the origin $\approx\omega\tau/2\pi$ times before absorption sets in.

The temporal behavior of the electric field in model (A) is indicated in Fig. 1(b).

The power spectrum P_A of the phase modulation in Eq. (1) may be obtained by taking its Fourier transform[7] analytically

$$P_A = (T_a/\omega')\{\exp[(\pi - 2\theta)\omega' T_a] - \exp[-(\pi + 2\theta)\omega' T_a]\}^{-1},$$

where ω' is the frequency shift from line center and $\theta = \arctan(\omega\tau)$ in the first quadrant. This is plotted in Fig. 1(c) for $\omega\tau = 2\pi$. Most of the energy is on the anti-Stokes side, since the plasma modulation up shifts the frequency.

For large frequency shifts the power spectrum falls off exponentially as indicated by the straight lines in the semi-log plot of Fig. 1(c). The fall off on the anti-Stokes side, $\sim\exp(-2\omega' T_a/\omega\tau)$, is much slower than the fall off on the Stokes side, $\sim\exp(-\pi\omega' T_a)$, at least when the collision frequency is less than the laser frequency, which is the usual case. The exponential fall off for large frequency shifts will prove to be typical not only of the two models (A) and (B), but also of the experimental results.

For small frequency shifts, the power spectrum reduces to $1/2\pi\omega'^2$, which is the power spectrum of a sudden step-function cutoff of the beam. This

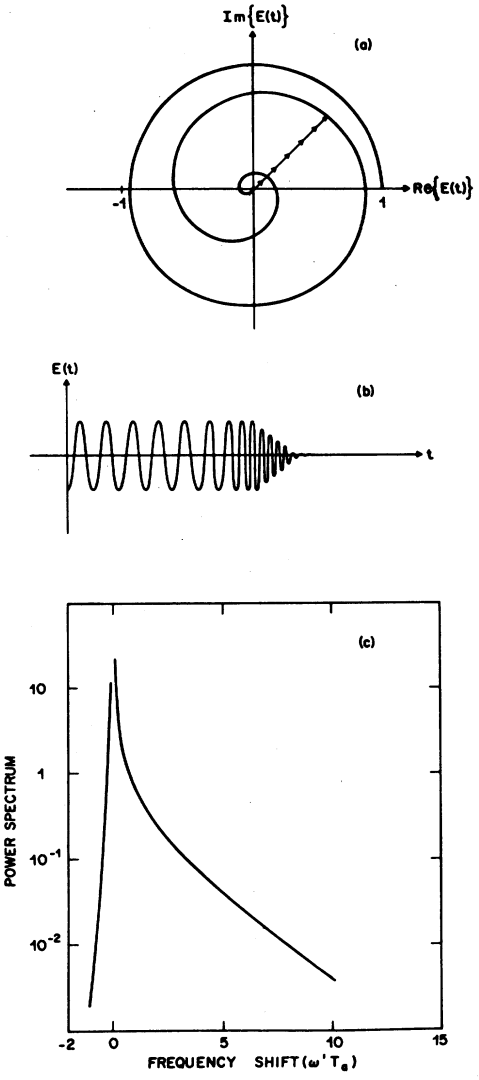

FIG. 1. (a) Electric field of model (A) when plotted in a phasor diagram. The line with the arrows is the electric vector of the light wave in the complex plane. Because of the phase modulation it follows a circular path as the plasma density builds up in time. Eventually, the plasma becomes opaque and the vector spirals in to the origin. (b) Qualitative behavior of a sine wave with the phase and amplitude modulation of model (A). Note that the frequency becomes upshifted. (c) Power spectrum of the modulation in model (A). The anti-Stokes side is much stronger than the Stokes side.

is reasonable, since small frequency shifts correspond to long times, and on a long-time scale the effect of the breakdown is simply to terminate transmission of the beam. This is precisely what is observed within the time resolution available on an oscilloscope.[4]

IV. MODEL (B)

In constructing model (B) we will avoid the main assumption of model (A), that of a homogeneous plasma. Of course, even if the plasma density started out uniformly, it would rapidly become spatially inhomogeneous, since the avalanche growth rate is a sensitive function of light intensity. In the focus the intensity is strongest at the center and falls off rapidly. Furthermore, there is no reason to believe that the plasma is initially uniform, since it probably nucleates at a specific point in space. These shortcomings will be corrected in model (B).

The primary effect of the assumption of a uniform plasma is to cause a uniform shift in phase of the light beam as a whole. Therefore the phase of the light wave may become much larger than 2π, and the electric vector will circle the origin of the phasor diagram, Fig. 1(a). This causes the anti-Stokes side of the spectrum to be very strong while the Stokes side becomes virtually insignificant. In the experimental spectra, it will be seen that the Stokes side of the spectrum, although relatively weak, is not as weak as predicted by model (A).

In a nonuniform plasma, on the other hand, different parts of the beam will experience a different phase shift. If a part of the beam is phase shifted more than 2π, then another part may be shifted less and the net resultant vector in the complex plane will cancel. In general, the path of the resultant vector will not circle the origin without experiencing almost complete cancellation. This physical situation is shown in Fig. 2(a). For model (B) let us assume that the tip of the resultant vector of the electric field follows an elliptical path to the origin. A physically reasonable example of such an electric field is

$$E(t) = \tfrac{1}{2}[1 - \tanh(t/\mathcal{T}) + i\epsilon/\cosh(t/\mathcal{T})] . \qquad (2)$$

It can be verified that Eq. (2) represents an ellipse in the complex plane with a ratio of the major to minor axis of $1/\epsilon$. The imaginary part of E describes phase modulation. If ϵ is set equal to zero, then model (B) reduces to the pure amplitude modulation model which had been considered in Ref. 4.

The temporal behavior of the electric field of model (B) is indicated in Fig. 2(b). The time required for the electric field amplitude to drop from its value before the spark formed to a negligible value afterward is $\sim 2.2\tau$.

The power spectrum P_B of Eq. (2) may again be obtained analytically

$$P_B = \frac{\pi \mathcal{T}^2}{8}\left(\frac{1}{\sinh(\frac{1}{2}\pi\omega'\mathcal{T})} + \frac{\epsilon}{\cosh(\frac{1}{2}\pi\omega'\mathcal{T})}\right)^2 .$$

This plotted in Fig. 2(c) for $\epsilon = 0.5$.

As before, the power spectrum for this model falls off exponentially at large frequency shifts.

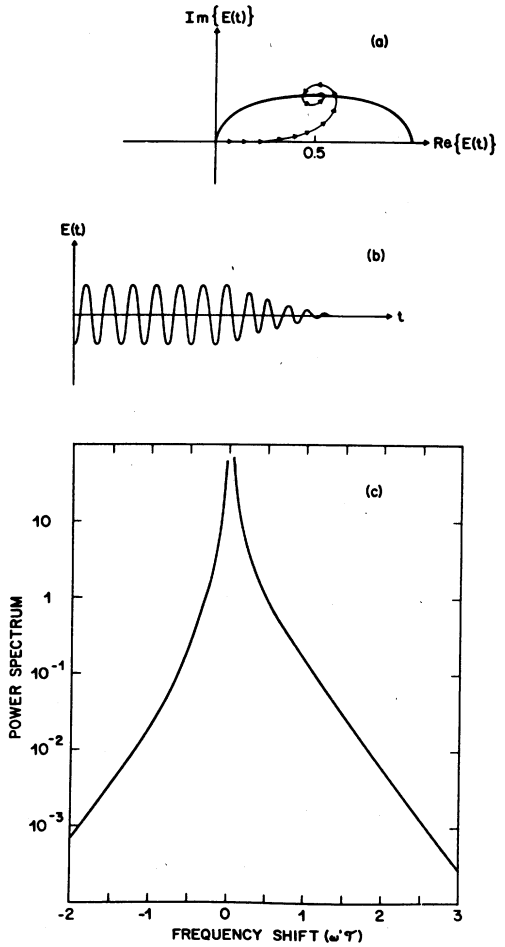

FIG. 2. (a) Electric field of model (B) when plotted in a phasor diagram. The line with the arrows is the vector sum of the various contributions to the output field of the light wave in the complex plane. Since the plasma is spatially inhomogeneous, each contribution enters with a slightly different phase angle. Consequently, the resultant vector follows an elliptical path to the origin as the plasma grows in space and time. (b) Qualitative behavior of a sine wave with the phase and amplitude modulation of model (B). The phase modulation is much less pronounced than in model (A). (c) Power spectrum of model (B).

This seems to be a characteristic feature of most realistic models, and is roughly corroborated by the experiments. The fall off on both the Stokes and anti-Stokes side is $\sim\exp(-\pi\omega'\tau)$ but the anti-Stokes side is stronger than the Stokes side by a factor $(1+\epsilon)^2/(1-\epsilon)^2$.

For small frequency shifts, the power spectrum again reduces to $1/2\pi\omega'^2$ which is the power spectrum of a sudden step function cutoff of the beam. This is a universal feature of any model for the same reasons which were already mentioned in connection with model (A).

These models, while too simple to provide a quantitative picture of the physical processes (a)–(d), will nevertheless guide us in interpreting the distinctive features of the experimental spectra.

V. EXPERIMENT

The basic experimental apparatus is shown in Fig. 3. The source is a Lumonics model 103 TEA (transverse electric atmospheric) CO_2 laser equipped with an unstable resonator cavity. The totally reflecting rear mirror has a concave radius of curvature of 4.57 m. The front mirror is made of germanium with a 0.75-m radius of curvature, concave on one side, convex on the other. Both sides are anti-reflection coated, except for a small 5-mm spot on the convex side which is left uncoated. This provides sufficient feedback for oscillation. The laser delivered about 10 MW in a diffraction limited output spot.

The focusing lens used in this experiment is all important. In order to achieve the maximum possible intensity at the focus, the lens should have diffraction limited performance, and a very low f number. The germanium doublet[8] used here is fully corrected for spherical aberration and has a speed $f/1$. It produces a focal spot only 17 μm in diameter. The optical correction was checked by using two lenses in series to focus and recollimate the beam, then verifying that the transmitted beam was still diffraction limited. The spherical aberration, which adds for two lenses in series, was therefore negligible.

In this experiment the laser spark was formed between two such lenses. Special measures were taken to ensure that the gas at the focus was free of impurities. These steps will be discussed in a later section. For the high-pressure measurements, the focusing lens was mounted in a brass cell with a 1-in. diameter 15-mm-thick germanium front window, able to withstand up to 100 atms.

The recollimating lens transmitted the light to the entrance slits of a 0.85-m Spex double monochromator. It was equipped with two 10-cm-wide diffraction gratings having 150 grooves/mm. The ultimate resolution of this instrument, 1 GHz, was confirmed by scanning the apparent laser linewidth.

A double spectrometer is very important in achieving the necessary rejection ratio for this experiment. In fact, if a single grating spectrometer is used, then the ratio of signal to elastically scattered background light from the grating is only about 1:1. It may be possible to improve upon this by using a diamond-shaped mask[9] on the grating to reduce the strength of the side lobes in its far-field diffraction image.

At the output slit of the monochromator is a liquid-helium-cooled Santa Barbara Research Corp. Ge:Hg photoconductor. The speed of the detector is about 400 MHz and the signal is transmitted, via a 50-Ω coaxial cable, from inside the Dewar to a high-speed oscilloscope. Both a Tektronix 7904 and a Tektronix 519 were used to observe the signal.

The signal consisted of a short spike of light, with a duration equal to the time resolution of the detection system, or about 1 nsec. This is shown in Fig. 4(a). The elastically scattered light within the spectrometer was many orders of magnitude weaker, and it could be distinguished from the signal because (a) it had the 100-nsec duration of the incident laser pulse and (b) it was present even when no breakdown occurred.

In some experiments, scattered light was intentionally introduced in order to confirm that the instant at which the plasma formed, cutting off transmission of the laser beam was the same instant at which the signal spike appeared.

Although the shape of the signal spike in Fig. 4(a) remains constant from shot to shot, its amplitude fluctuates greatly. This is not surprising, since the incident laser intensity at which the plasma nucleates also fluctuates greatly from shot to shot. The fluctuations in spike amplitude are somewhat greater, however. The shape of the spike is simply the response function of the detection system to a δ-function impulse, and is therefore unchanged from shot to shot.

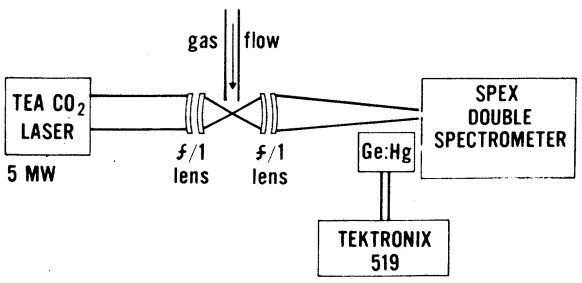

FIG. 3. Experimental apparatus.

When the slits of the spectrometer were opened wide, the spike narrowed in time as shown in Fig. 4(b). This is a direct verification of the uncertainty principle for time and frequency. It is made possible because the 1-GHz speed of the Tektronix 519 oscilloscope just overlaps the 1-GHz resolution of the double spectrometer. An equivalent explanation of this effect is to say that the pulse stretching in Fig. 4(a) is caused by the differential path delay between light which is diffracted from the near and far edges of the grating. In the spectrometer used here, the overall differential delay is 1 nsec, which is within the time resolution of the detection system.

The Ge:Hg photoconductor has 1-nsec recombination time, which is actually longer than the rise time of 370 psec in Fig. 4(b). Therefore, the photoconductor is acting as an integrator. Thus, the optical pulse is certainly shorter than 370 psec. The rise time is also limited by the oscilloscope (300 psec) and the RC product of the detector element. Therefore we can place an upper limit of 300 psec on the optical pulse duration. The fall time of the electrical pulse is given by the recombination time and the wiggles on the tail are due to ringing in the transmission line caused by the high-speed transient.

VI. RESULTS

The energy of the optical pulse in Fig. 4 was measured as a function of frequency shift from the incident laser. The resulting spectra are shown in Fig. 5. Since the pulse energy is normalized in terms of the incident laser power, the appropriate units[7] are picoseconds per unit wave number.

In Fig. 5(a) is shown the result for the breakdown spectrum of nitrogen gas at 1 atm. In the low frequency region, within about $\omega' \sim 1\ \mathrm{cm}^{-1}$ of

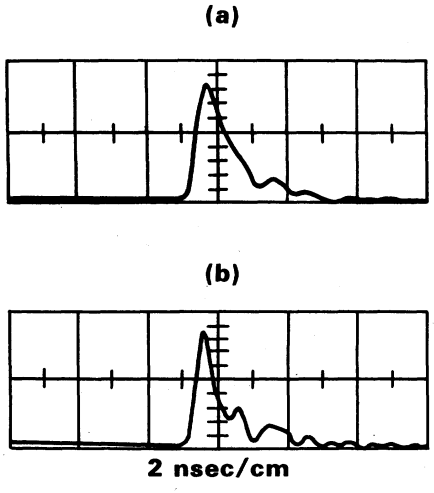

FIG. 4. (a) Signal spike observed on a Tektronix 519 oscilloscope with the spectrometer slits narrowed for maximum frequency resolution. (b) Signal spike observed with the spectrometer slits wide open. The pulse stretching of (a) is a direct consequence of the uncertainty principle for time and frequency.

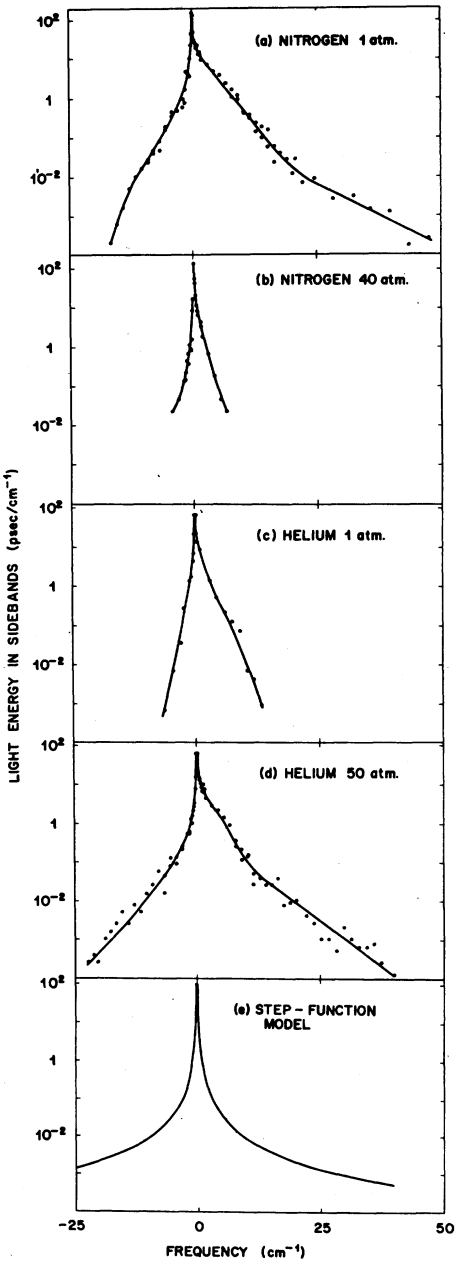

FIG. 5. (a)–(d) Power spectra produced by breakdown and self-phase modulation in nitrogen and helium gas at various pressures. (e) Power spectrum $1/2\pi\omega'^2$ produced by an instantaneous step-function termination of a light beam. Note that the units on the ordinate axis are picoseconds per wave number. (See Ref. 7.)

the laser line, the spectrum is symmetric, and agrees with the $1/2\pi\omega'^2$ power spectrum of a step-function modulation, Fig. 5(e). This indicates that the beam is cut off in a time of $1/\omega' \sim 30$ psec. Beyond a 1-cm^{-1} frequency shift, the spectrum becomes asymmetrical with about 10 times more energy on the anti-Stokes than on the Stokes side. This is quite naturally expected from the phase modulation due to a negative index change Δn. Additionally the spectra seem to fall off roughly exponentially, as predicted by models (A) and (B).

With the pressure increased to 40 atm of nitrogen the spectrum becomes weaker and narrower. The Stokes side is especially reduced, and the spectrum is asymmetric even for small frequency shifts, indicating that the beam is cut off rather slowly.

Surprisingly, the influence of pressure on the strength of the spectrum is opposite in helium and nitrogen. The far wings of the spectrum in helium are much stronger at 50 atm, Fig. 5(d), than at 1 atm, Fig. 5(c). Meanwhile, at small frequency shifts, the spectra are symmetric at both high and low pressures, and the step-function model, Fig. 5(e), is satisfactory.

Clearly the wide range of physical behavior observed in Figs. 5(a)–5(d) is too complicated to be explained by the models (A) and (B). Nevertheless, certain over-all features stand out distinctly. High-pressure nitrogen excepted, the low-frequency behavior is well described by the step function model, at least within ~1 cm^{-1} of the laser line. Therefore the beam is cut off in a time ~30 psec. If this is interpreted as the time required for the plasma to spread across the focal region, then the speed of the plasma front is $\sim 10^8$ cm/sec.

The far wings of the spectra, while they are in qualitative accord with models (A) and (B), actually contain too much energy. The discrepancy is particularly noticeable in low-pressure nitrogen, Fig. 4(a), and high-pressure helium, Fig. 4(d). This indicates that there is considerable high-frequency phase structure induced on the light beam in a time scale between $\lesssim 1$ and 30 psec, corresponding to frequency shifts between 50 and 1 cm^{-1}.

VII. DISCUSSION

One of the problems in the measurement of the spectra in Fig. 5 is the uncertainty in the nucleation mechanism for the plasma. The laser intensities used here, $\gtrsim 10^{12}$ W/cm^2, exceed by many orders of magnitude the avalanche thresholds[10] of the gases used. Therefore we can say with certainty that there were no initiating electrons available in the focus until the instant of nucleation.

For the self-phase modulation to give a measurable frequency shift the rate of plasma growth should be very fast. Since this rate increases with the incident light flux, an effort is made to transmit the maximum possible intensity before the instant of nucleation. The gas is kept clean by flowing it rapidly through the focal region, Fig. 3. Secondly, the focal volume is kept small by using a lens of low f number. This helps reduce the probability of having an impurity in the high intensity region.

In order to ascertain the nucleation mechanism, filters[11] with a pore size of ~100 Å were placed in the gas line. It was found that the mean intensity for breakdown increased about a factor of 2. This indicates that the plasma nucleates on small dust particles or large molecules in the 100-Å range. The uncertainty in the availability of a nucleation center near the focal region is probably responsible for the shot to shot fluctuations. Thus, not only the intensity at nucleation, but especially the resulting self phase modulation spectrum, changes on each shot. Therefore, no single model would be completely adequate in interpreting the results.

To handle the fluctuations in a consistent way the following procedure was used. Each experimental point in Fig. 5 is the peak amplitude of the signal observed from 20 successive laser shots. The line drawn through the points is therefore the "envelope" of the peak values occurring in 20 successive spectra. It may be desirable to repeat this experiment with a visible laser and record the entire spectrum on photographic film in a single shot. An even more desirable alternative is to eliminate the fluctuations in the nucleation mechanism altogether.

If the laser intensity is high enough, direct electron tunnelling may produce the initial electron of the avalanche. Since the tunnelling probability[12] is a very sensitive function of electric field, the plasma will tend to nucleate at a well defined intensity in the center of the focal region. Thus it is possible to eliminate the fluctuations in the nucleation mechanism if the 10^{14}-W/cm^2 intensity required for electron tunnelling could be achieved. There are other reasons for trying to attain such a high intensity. One may anticipate that the ionization potential would be strongly Stark shifted. Also, the rate of plasma growth would be very high, since such an energy flux is sufficient to ionize all the atoms in the focal region within only a few optical cycles.

As mentioned earlier, particles in the 100-Å range were found to be limiting the breakdown intensity to ~10^{12} W/cm^2. There was only a factor-of-2 improvement when the finest available gas filters[11] were used. To further increase the nucleation intensity, the boil-off vapors of liquid ni-

trogen and liquid helium were flowed through the focus, reasoning that these vapors were the cleanest possible source of gas. The intensity rose to near 10^{13} W/cm^2, a dramatic improvement, but still not enough. The breakdown was still being initiated at impurities since the nucleation intensity was changing from shot to shot. Reproducibility of the signal spikes was greatly improved, however, with fluctuations not much larger than those observed in the incident intensity. This reproducibility improvement was especially noticed in the far wings of the spectrum, which were followed to larger frequency shifts than was possible before.

There are other techniques for improving the reproducibility, but which involve an artificially introduced nucleation mechanism. For example, a spark plug could be fired near the focus at the instant when the laser intensity reaches a predetermined level. Ionizing radiation from the spark[13] would provide initiating electrons for the laser produced plasma. Another scheme is to dope the clean gas with an impurity from which electron tunnelling occurs at 10^{12} W/cm^2. Then the plasma would nucleate reproducibly, though possibly not at as high an intensity as desired.

Understandably, the rewards for further cleaning up the gas are very high. In addition to the improved reproducibility, the plasma growth will become fast enough to produce light pulses only a few optical cycles in duration.

VIII. SHORT-PULSE GENERATION

The basic concept[4] of short pulse generation from a laser spark is to employ a spectral filter which rejects the incident laser wavelength, but transmits the sidebands produced by the sudden plasma growth. Among the types of spectral filters which have been suggested are the Michelson interferometer,[14] the Fabry-Perot etalon,[15] the grating monochromator[3,4] and most recently, resonant material absorbers.[5] Of these, the latter two schemes have the important practical advantage of a high rejection ratio.

Since the spectral filters are basically passive elements, it is advantageous to use linear systems analysis to understand their behavior. Let $E(\omega')$ be the Fourier amplitude of the spectrum induced by the laser spark, and let $G(\omega')$ be the transmittance function of the spectral filter. The electric field of the output pulse in the time domain is the inverse Fourier transform of the product $E(\omega')G(\omega')$. Both the real and imaginary parts of the transmittance function must be included to avoid violating causality. To ensure a high rejection ratio, $G(0)$ should be very small.

The output pulse in time, may also be written using the convolution theorem

$$E_{\text{out}} = (2\pi)^{-1/2} \int_{-\infty}^{\infty} E(t')g(t-t')\,dt', \tag{3}$$

where $E(t')$ is the electric field produced by the laser spark and $g(t-t')$ is the Fourier transform of the transmittance function of the spectral filter, or equivalently, its response to a δ-function input pulse. Therefore g is a type of Green's function for the system. For example, in the physically important[5,16] case of a Lorentzian absorber

$$g(x) = \exp\left(i\Delta\omega x - \frac{x}{T_2}\right)\left(\frac{\pi M}{xT_2}\right)^{1/2} J_1\left(\left(\frac{2Mx}{T_2}\right)^{1/2}\right)$$

where T_2 is the homogeneous relaxation time of the absorber, $\Delta\omega$ is the difference between the laser frequency and the center of the absorption line, M is the maximum absorption in nepers, and J_1 is the Bessel function of the first kind of order 1.

If the effect of the breakdown can be regarded simply as a step-function cutoff of the electric field, then Eq. (3) simplifies

$$E_{\text{out}} = (2\pi)^{-1/2} \int_{-\infty}^{0} g(t-t')\,dt'. \tag{4}$$

From Eq. (4), we see directly that the output pulse shape is entirely determined by the linear response of the spectral filters. This generalization is true only on a time scale longer than the fall time of the transmitted light ≈30 psec. On a shorter time scale, it would be necessary to use Eq. (3) and substitute the full phase and amplitude structure of the electric field. Unfortunately, this fluctuates from shot to shot and we have no way of measuring it. Therefore, only pulses 30 psec and longer were reliably generated by the techniques described here. Further cleanup of the gas will be necessary for going to shorter times, as was amply discussed in Sec. VII.

It is reasonable to ask, what additional considerations are important for producing shorter pulses, especially in the range of only one or two cycles. Clearly, such a pulse requires a spectrum as broad as the laser frequency itself, with the highest and lowest frequencies differing by an octave. This can be provided by the spark if it terminates the beam quickly enough.

The Fourier amplitude of a step-function modulation is $E(\omega') \sim 1/\omega'$. An *ideal* matched filter has transmittance function $G(\omega')$ proportional to ω'. Notice that $G(0) = 0$ and that the product $E(\omega')G(\omega')$ would be constant, independent of frequency. Therefore, a δ function in time would be generated, with a duration limited only by its reciprocal frequency width and a peak power equal to the inci-

dent power.

A good approximation to the *ideal* filter $G(\omega')$, is a $\frac{1}{4}$ wave antireflection coated surface used in reflection. In practice however, such a filter is not really necessary. A multilayer dielectric filter, which transmits only the far wings of the breakdown induced spectrum would be sufficient because the far wings contain most of the high speed temporal structure, and $1/\omega'$ has only slow variation with ω' at large ω'.

A more serious problem for short pulse generation and propagation is pulse stretching due to index dispersion. This difficulty is of course common to all schemes for producing short pulses. Fast pulses inherently contain many frequency components. Upon propagation through a dispersive medium, the high- and low-frequency components fall out of step, and the pulse is stretched in time. It may be shown, by convolving the Fourier amplitude of a short pulse with a propagation factor containing a quadratic contribution to the phase, that only pulses longer than $\sim[(z/c)dn/d\omega]^{1/2}$ may propagate without stretching. Here z is the propagation thickness and c is the speed of light.

For the pulse generating techniques described here, dispersion in the recollimating lens and in the spectral filter may have a deleterious effect. Fortunately, infrared optical materials have rather low dispersion near the CO_2 laser frequency, and a pulse of only a few optical cycles may be transmitted through several millimeters of germanium without distortion. In the visible region, such favorable window materials do not exist, and it may be necessary to compensate the dispersion with a grating pair.[17]

In conclusion, it will be possible to generate pulses consisting of only a few optical cycles if the following problems are overcome: (i) The rate of plasma growth in the focal region must be speeded up. This will probably require a gas which is so clean that the plasma will not nucleate until the intensity is $\sim 10^{14}$ W/cm^2. (ii) The undesirable dispersion of the optical components must either be eliminated or compensated.

In the picosecond regime, these problems are solved, and the techniques described in this paper are already generating clean, predictable, and reproducible optical transients.[5] These methods are unique in that the temporal pulse shape and duration are *analytically* determined by the *linear* optical properties of a passive filter.

I would like to acknowledge the valuable ideas which were contributed by J. Goldhar, M. Duguay, N. Bloembergen, and W. F. Brinkman.

---

*Present address: Gordon McKay Laboratory, Harvard University, Cambridge, Mass. 02138.

[1]P. D. Maker, R. W. Terhune and C. M. Savage, in *Proceedings of the Third International Conference on Quantum Electronics*, edited by P. Grivet and N. Bloembergen (Dunod, Paris, 1964), pp. 1559–1576.

[2]Eli Yablonovitch and N. Bloembergen, Phys. Rev. Lett. 29, 907 (1972); N. Bloembergen, Optics Commun. 8, 285 (1973).

[3]Eli Yablonovitch, Phys. Rev. Lett. 32, 1101 (1974).

[4]Eli Yablonovitch, Phys. Rev. Lett. 31, 877 (1973).

[5]Eli Yablonovitch and J. Goldhar, Appl. Phys. Lett. (to be published).

[6]V. L. Ginzburg, *The Propagation of Electromagnetic Waves in Plasmas*, 2nd ed. (Pergamon, Oxford, 1970).

[7]All the power spectra in this paper are normalized to unit incident laser power (i.e., the incident power before the spark forms). Therefore, the natural units of a power spectrum, energy per unit wave number, become units of picoseconds per unit wave number when normalized.

[8]This lens is manufactured by Laser Optics Inc., Danbury, Conn.

[9]Spex Industries, Inc. (private communication).

[10]Eli Yablonovitch, Appl. Phys. Lett. 23, 121 (1973).

[11]Filters from Millipore Corp., Gelman Instrument Co., and Nuclepore Corp., were employed, all with similar results.

[12]L. V. Keldysh, Zh. Eksp. Teor. Fiz. 47, 1945 (1964) [Sov. Phys.—JETP 20, 1307 (1965)].

[13]H. J. Seguin, J. Tulip and D. C. McKen, IEEE J. Quantum Electron. QE-10, 311 (1974).

[14]A. Szoke, J. Goldhar, H. P. Grieneisen, and N. A. Kurnit, Opt. Commun. 6, 131 (1972).

[15]M. Duguay (private communication).

[16]M. D. Crisp. Phys. Rev. A 1, 1604 (1970).

[17]E. B. Treacy, IEEE J. Quantum Electron QE-5, 454 (1969).